

1 *Type of the Paper (Article)*

2 **High-performance SiC-polycrystalline fiber with** 3 **smooth surface**

4 **Ryutaro Usukawa**¹, **Toshihiro Ishikawa**²

5 ¹ Tokyo University of Science, Yamaguchi; F118701@ed.tusy.ac.jp

6 ² Tokyo University of Science, Yamaguchi; ishikawa@rs.tusy.ac.jp

7 * Correspondence: ishikawa@rs.tusy.ac.jp; Tel.: +81-836-88-4564

8

9 **Abstract:** Polymer-derived SiC-polycrystalline fiber (Tyranno SA) shows excellent heat-resistance
10 up to 2000°C, and relatively high strength. Up to now, through our research, the relationship
11 between the strength and residual defects of the fiber, which were formed during the production
12 processes (degradation and sintering), has been clarified. In this paper, we addressed the
13 relationship between the production condition and the surface roughness of the obtained
14 SiC-polycrystalline fiber, using three different raw fibers (Elementary ratio: Si₁Al_{0.01}C_{1.5}O_{0.4-0.5}) and
15 three different types of reactor (Open system, Partially-open system, and Closed system). With
16 increase in the oxygen content in the raw fiber, the degradation during the production process
17 easily proceeded. In this case, the degradation reactions (SiO+2C=SiC+CO and SiO₂+3C=SiC+2CO)
18 in the inside of each filament become faster, and then the CO partial pressure on the surface of each
19 filament is considered to be increased. In consequence, according to Le Chatelier's principle, the
20 surface degradation reaction and grain growth of formed SiC crystals would be considered to
21 become slower. That is to say, using the raw fiber with higher oxygen content and closed system
22 (highest CO content in the reactor), much smoother surface of the SiC-polycrystalline fiber could be
23 achieved.

24 **Keywords:** SiC-polycrystalline fiber; Defect; Strength; Surface roughness

25

26 **1. Introduction**

27 Since the first precursor ceramics using polycarbosilane was developed, lots of polymer-derived
28 SiC-base fibers have been developed. Present commercial polymer-derived SiC fibers are shown in
29 Table 1. Through these developments, the heat-resistances of the SiC-based fibers were remarkably
30 increased from 1300°C to 2000°C as can be seen from this table. Of these fibers, SiC-polycrystalline
31 fibers (Tyranno SA, Hi-Nicalon Type S, and Sylramic) show the highest heat-resistance up to 2000°C,
32 and then have been actively evaluated for aerospace applications as SiC/SiC composites [1-5].
33 However, to extend the application field, increase in the fiber's strength is eagerly required. Up to
34 now, through our research, the relationship between the strength and the residual defects contained
35 in the fiber, which were formed during the production processes, has been clarified [6-9]. In these
36 researches, we have proposed several new methods for reducing the residual defects, and also
37 demonstrated them using the conversion process from amorphous Si-Al-C-O fiber to
38 SiC-polycrystalline fiber (Tyranno SA). Tyranno SA is produced by heat-treatment processes of
39 amorphous Si-Al-C-O fiber which is synthesized from polyaluminocarbosilane [1]. During the
40 heat-treatment processes, a degradation of the Si-Al-C-O fiber and a subsequent sintering of the
41 degraded fiber proceed as well, accompanied by a release of CO gas and compositional changes, to
42 finally obtain the dense structure. Since these structural changes proceed in each filament, a strict
43 control should be needed to minimize residual defects. As mentioned above, to reduce the residual
44 defects, we proposed new conversion processes and demonstrated them [7-9].

45

Table 1. Commercial Polymer-derived SiC Fibers

	Fiber's Grade	Manufacturer	
First Generation ~1300°C	Nicalon NL 200	NGS ^(~2012) (Nippon Carbon)	Amorphous
	Tyranno Lox M	UBE	
	Tyranno S	UBE	
Second Generation ~1500°C	Hi-Nicalon	NGS ^(~2012) (Nippon Carbon)	Amorphous
	Tyranno ZMI	UBE	
Third Generation ~2000°C	Hi-Nicalon Type S	NGS ^(~2012) (Nippon Carbon)	SiC-Polycrystalline
	Tyranno SA	UBE	
	Sylramic	COIC	

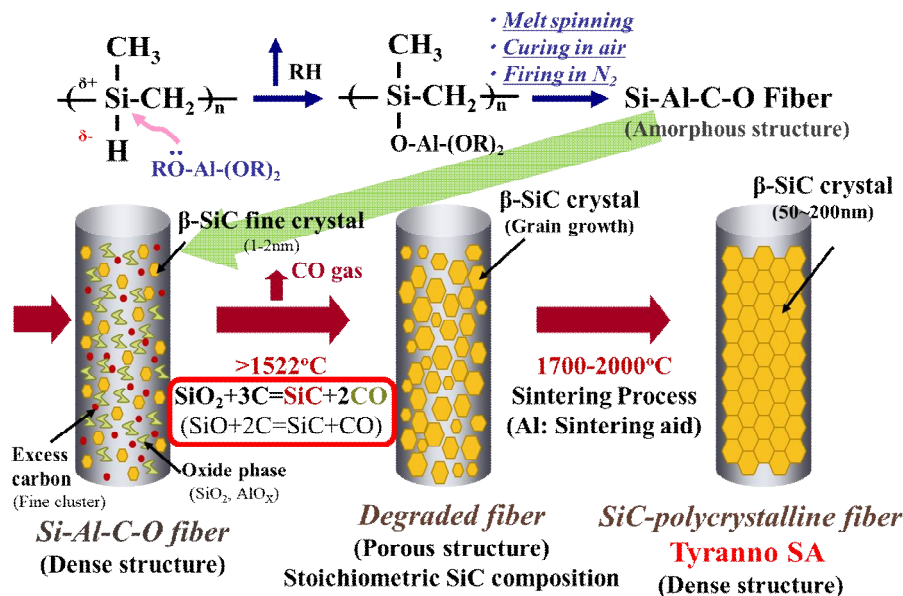
46

47 And then, using these new processes, the inside defects were remarkably reduced. As the result
 48 of these research, the present maximum strength of the improved fiber is ~4GPa. However, this
 49 strength is remarkably low compared with a theoretical strength (46GPa) of SiC crystal which can be
 50 calculated using Orowan's equation [10]. Accordingly, further improvement will be needed. In the
 51 above research, by controlling the advantageous degradation-reaction and preventing the
 52 disappearance of gaseous SiO from each filament, residual carbon (one of residual defects) was
 53 remarkably reduced along with prevention of abnormal surface grain growth. In consequence, the
 54 surface roughness was relatively improved compared with that of previous fibers. By the way, the
 55 surface roughness was very sensitive depending on the atmospheric condition during the
 56 degradation process, and then obtaining much smoother surface was a relatively difficult problem.
 57 Smoother surface of the fiber is very important for obtaining good fibrous fracture behavior of
 58 ceramic matrix composites (CMCs) [11]. Accordingly, it should be important to clarify the
 59 relationship between the process condition and the surface roughness of the obtained fiber. Here, we
 60 describe the formation mechanism of the surface structure and the relationship between the process
 61 condition and the surface roughness of the obtained SiC-polycrystalline fiber.

62 2. Materials and Methods

63 The SiC-polycrystalline fiber (Tyranno SA) was synthesized by heat-treating an amorphous
 64 Si-Al-C-O fiber up to 2000°C in argon gas atmosphere. The Si-Al-C-O fiber was produced from
 65 polyaluminocarbosilane which was synthesized by a reaction of polycarbosilane with
 66 tetra-butoxyaluminum at 300°C in nitrogen atmosphere. A spun fiber was obtained by
 67 melt-spinning of the polyaluminocarbosilane, and then the spun fiber was cured at around 200°C in
 68 air. The cured fiber was fired at 1300°C in nitrogen atmosphere to obtain the amorphous Si-Al-C-O
 69 fiber which was composed of SiC fine crystals, oxide phases (estimated forms: SiO₂, AlO_x), and
 70 excess carbons. By the way, as mentioned above, since in this synthesis we used
 71 polyaluminocarbosilane which was synthesized by the reaction of polycarbosilane and
 72 tetra-butoxyaluminum, we presumed that the aluminum existed as some oxide forms in the
 73 Si-Al-C-O fiber. In the next step, the amorphous Si-Al-C-O fiber was heat-treated up to 1500°C in
 74 argon gas atmosphere. During the heat-treatment, by the existence of the oxide phase and excess
 75 carbon in the fiber, the amorphous Si-Al-C-O fiber was degraded accompanied by a release of CO
 76 gas to obtain a porous degraded fiber. The porous degraded fiber was composed of a nearly
 77 stoichiometric SiC composition containing small amount of aluminum. In this case, since a part of
 78 the aluminum contained in the amorphous Si-Al-C-O fiber might be disappeared as some oxide

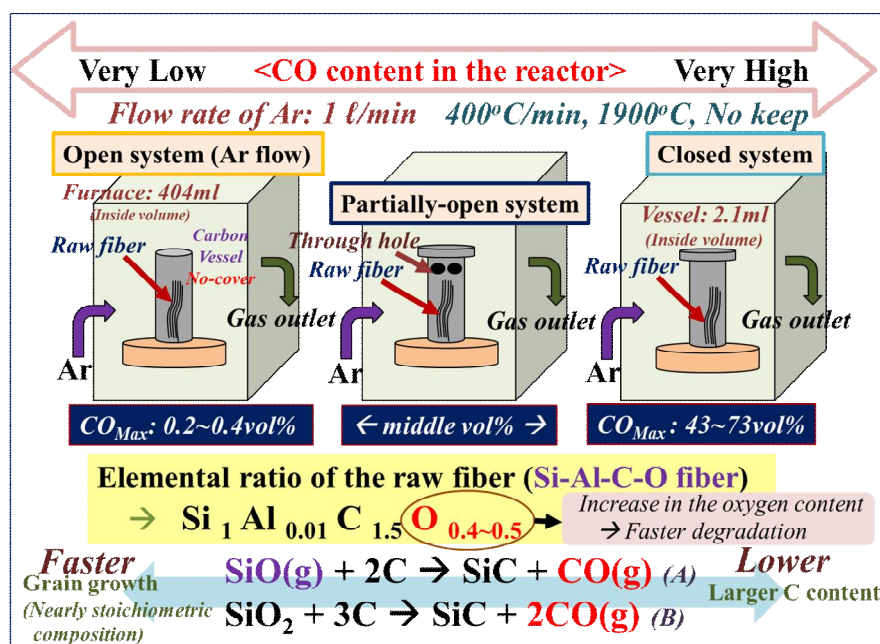
79 materials during the heat-treatment process, consequently a very small amount of aluminum (less
 80 than 1wt%) was contained in the degraded fiber. By the existence of the small amount of aluminum,
 81 at the next step, an effective sintering proceeded in each degraded filament composed of the nearly
 82 stoichiometric SiC crystals during further heat-treatment up to 2000°C in argon atmosphere. The
 83 production scheme of the polymer-derived SiC-polycrystalline fiber using the Si-Al-C-O fiber as the
 84 raw fiber is shown in Fig.1.



85
 86
 87
 88
 89
 90
 91
 92
 93
 94

Fig.1 The production scheme of the SiC-polycrystalline fiber using a raw Si-Al-C-O fiber

As mentioned in our previous papers, degradation reactions of the amorphous Si-Al-C-O fiber enclosed in red frame in this figure (Fig.1) strongly affects the final fine-structure (inside structure and surface roughness) of the SiC-polycrystalline fiber. Especially, reaction condition concerning CO gas content during the degradation process is most important [6, 9]. Accordingly, in this research we adopted three types of reaction vessel (Open system, Partially-open system, and Closed system) made of carbon shown in Fig.2.



95
 96
 97

Fig.2 Experimental condition for research on fiber's surface roughness

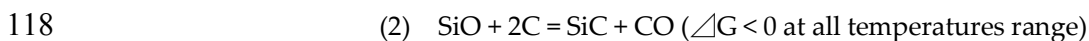
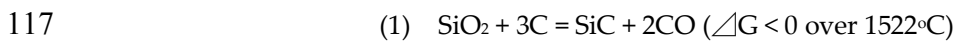
98 For the heat-treatment (degradation reactions and sintering) of the Si-Al-C-O fiber, we used
 99 "Super High Temperature Inert Gas Furnace (NEWTONIAN Pascal-40, Produced by NAGANO)"
 100 under argon gas flow (1 L/min). The size of the heating zone (made of graphite and C/C composites)
 101 is 35 mm in diameter and 40 mm in height. Several types of raw fibers (about 10 mg) (Elementary
 102 ratio: $\text{Si}_{11}\text{Al}_{0.01}\text{C}_{1.5}\text{O}_{0.4-0.5}$) were used and located in each vessel. The programming rate and the
 103 maximum temperature were $400^{\circ}\text{C}/\text{min}$ and 1900°C , respectively.

104 The surfaces and cross sections of the obtained fibers were observed using a field emission
 105 scanning electron microscope (FE-SEM), model JSM-700F (JEOL, Ltd.). Parts of surface region and
 106 inside of the several samples were sharpened by an etching machine using focused ion beam (FIB),
 107 and then the fine structures were observed by the transmission electron microscope (TEM), model
 108 JEM-2100F (JEOL, Ltd.). Surface roughness was observed using Atomic Force Microscope (AFM),
 109 model AFM 5000II (Hitachi, Ltd.).

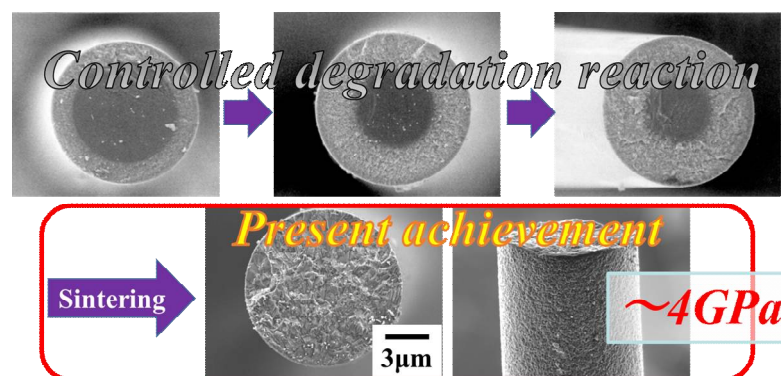
110 3. Results and discussion

111 3.1. Morphological changes during the degradation process

112 As mentioned before, for obtaining the SiC-polycrystalline fiber, at the first step, the amorphous
 113 Si-Al-C-O fiber was heat-treated up to 1500°C in argon gas atmosphere. During the heat-treatment
 114 process, by the existence of the oxide phase and excess carbon in the fiber, the amorphous Si-Al-C-O
 115 fiber was degraded accompanied by a release of CO gas to obtain a porous degraded fiber. This
 116 degradation of the Si-Al-C-O fiber proceeds mainly by the following two types of reactions.



119 The porous degraded fiber was composed of a nearly stoichiometric SiC composition containing
 120 small amount of aluminum (less than 1 wt%). By the existence of the small amount of aluminum, at
 121 the next step, an effective sintering proceeded in each degraded filament composed of the nearly
 122 stoichiometric SiC crystals during further heat-treatment up to 1900°C in Ar gas atmosphere. And
 123 then, the dense SiC-polycrystalline fiber was obtained. The morphological changes of each filament
 124 during the heat-treatment process (degradation and sintering) are shown in Fig.3.

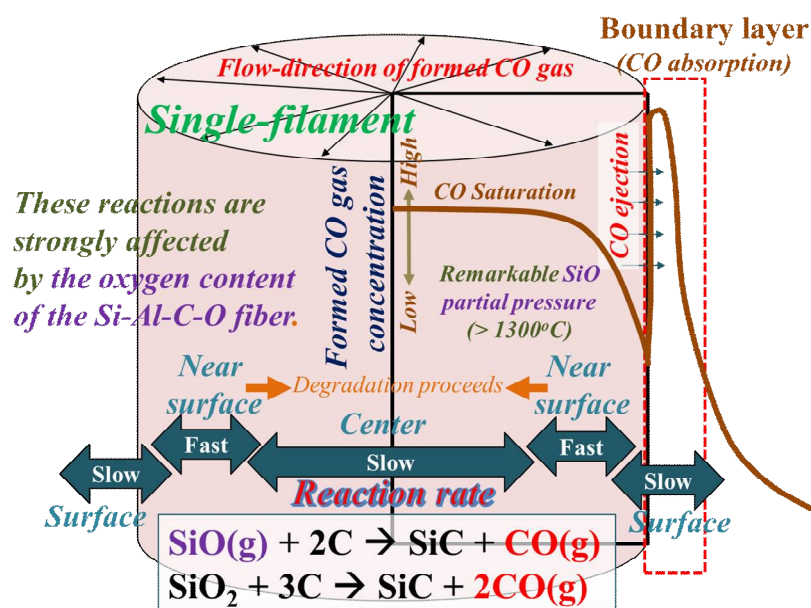


125

126 Fig.3 Morphological changes during the degradation and sintering processes

127 As can be seen from this figure (Fig.3), the degradation proceeded from outside to inside of the
 128 amorphous Si-Al-C-O fiber. And, regarding the SiC-crystalline size of the obtained sintered fiber, the
 129 surface SiC-crystals were relatively small compared with the inside crystals. This phenomenon was
 130 considered to be caused by the atmospheric condition (Especially: CO gas content) during the
 131 degradation process. That is to say, the degradation reactions ($\text{SiO}_2 + 3\text{C} = \text{SiC} + 2\text{CO}$ and $\text{SiO} + 2\text{C} =$
 132 $\text{SiC} + \text{CO}$) are strongly dominated by the CO gas content in the reactor. According to Le Chatelier's

133 principle, the higher the CO content becomes, the slower the reaction becomes. Anyway, the
 134 abovementioned degradation proceeds in the inside of each filament accompanied by a release of
 135 CO gas. So, the inside of each filament is saturated by the formed CO gas, and the surplus CO gas is
 136 ejected from the surface region to the outside. Furthermore, on the surface region of each filament,
 137 some boundary layer composed of CO gas must be formed. By these changes, in consequence, some
 138 CO gas distribution would be formed from the inside to the surface region of each filament.
 139 Accordingly, the degradation in the inside of each Si-Al-C-O filament was considered to proceed as
 140 shown in Fig.4.



141

142

Fig.4 General degradation in the inside of each Si-Al-C-O filament

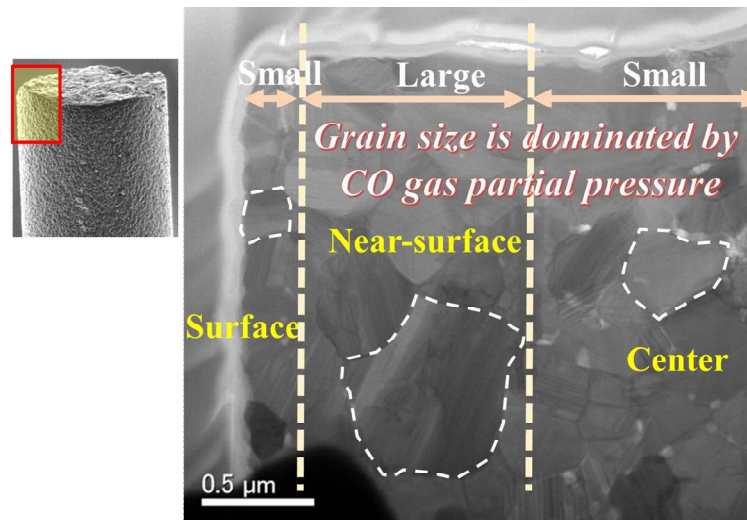
143 This figure shows general degradation reaction in the inside of the raw Si-Al-C-O filament.
 144 Degradation reaction proceeds according to the following reactions at high temperature:



147 These reaction-rates are dominated by the partial pressure of the formed CO gas. When these
 148 reactions proceed in each filament, the inside of each filament is saturated by the formed CO gas.
 149 However, from the surface region, the formed CO gas is ejected. Accordingly, the CO partial
 150 pressure of the near-surface region becomes lower compared with that of the inside. So, the reaction
 151 rate becomes lower at the center of each filament, compared with that of the near surface region. On
 152 the other hand, on the surface of the raw fiber, a boundary layer composed of CO gas is formed. In
 153 consequence, at the surface, CO gas concentration becomes relatively higher compared with that of
 154 the inside. These CO gas-balance dominates the fine structures of the obtained SiC-polycrystalline
 155 fiber. Regarding the above phenomena, a TEM image of the sliced cross-section of the obtained
 156 SiC-polycrystalline fiber is shown in Fig.5. As can be seen from this figure, the grain size
 157 (white-dotted line shown in Fig.5) at each position was different from each other. As mentioned
 158 above, the degradation rate and the obtained grain-size are dominated by the partial pressure of the
 159 formed CO gas. That is to say, CO gas concentration of the near-surface region of the fiber is
 160 relatively low compared with that of the inside, so that the reaction rate becomes higher to lead to

161 larger grain size compared with that of the inside. Furthermore, since the boundary layer composed
 162 of the ejected CO gas was formed on the surface, the partial pressure of CO gas on the surface

163 becomes higher to result in the smaller grain size. Considering these fundamental matters, we can
 164 control the surface roughness. In the next section, we will address the relationship between the
 165 degradation reaction at the surface and the surface roughness of the obtained SiC-polycrystalline
 166 fiber.

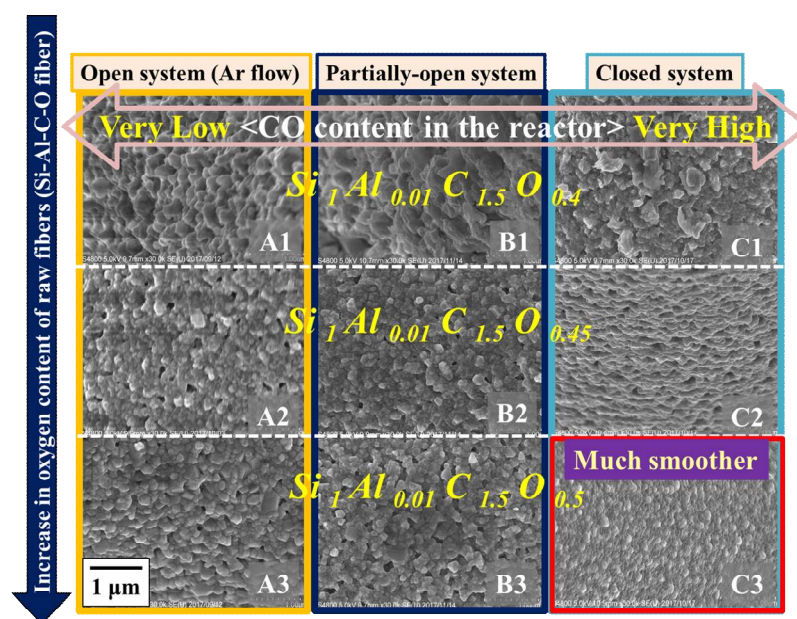


167

168 Fig.5 TEM image of the sliced cross-section of the obtained SiC-polycrystalline fiber

169 3.2. Change in the surface roughness of the SiC-polycrystalline fiber

170 As mentioned above, both the degradation reaction and the grain growth of the formed SiC
 171 crystals are strongly affected by the CO content in the reactor during the degradation reaction. As
 172 shown in Fig.2, we used three different types of vessel (Open system, Partially-open system, and
 173 Closed system) and several types of raw fiber (Elementary ratio: $\text{Si}_1\text{Al}_{0.01}\text{C}_{1.5}\text{O}_{0.4-0.5}$) for changing
 174 actual CO content in the reactor. Under our reaction condition, we calculated that the maximum CO
 175 content in the reactor was 73vol% when we used both the closed system and the raw fiber with
 176 highest oxygen content ($\text{Si}_1\text{Al}_{0.01}\text{C}_{1.5}\text{O}_{0.5}$), whereas the minimum CO content was 0.2vol% when we
 177 used both the open system and the other raw fiber with lowest oxygen content ($\text{Si}_1\text{Al}_{0.01}\text{C}_{1.5}\text{O}_{0.4}$). The
 178 surface structures (FE-SEM images) of the obtained SiC-polycrystalline fibers are shown in Fig.6.

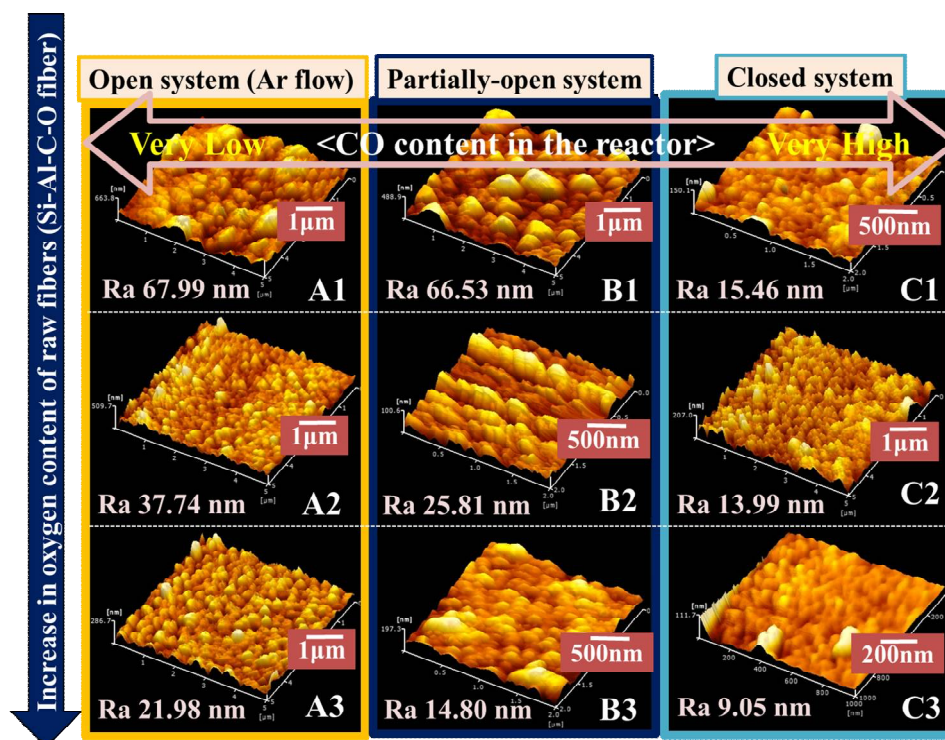


179

180 Fig.6 Changes in the surface structures obtained using different types of raw fiber and vessels

181 These fibers were obtained by heat-treatment of the different types of Si-Al-C-O fiber at 1900°C
 182 in Ar using the three different types of vessels. As can be seen from this figure (Fig.6), the higher the
 183 oxygen content of Si-Al-C-O fiber becomes, the smoother the surface becomes. These results are
 184 closely related to the CO content in the reactor during the degradation reaction. The much smoother
 185 surface was obtained using the raw fiber with highest oxygen content ($\text{Si}_{1.1}\text{Al}_{0.01}\text{C}_{1.5}\text{O}_{0.5}$) and the closed
 186 system. As can be seen from these results, the surface roughness is effectively controllable by
 187 changing the degradation conditions (Especially; CO content in the reactor). The most important
 188 factors for change in the CO content in the reactor are (1) Oxygen content of the raw Si-Al-C-O fiber,
 189 and (2) Reactor system (Open system, Partially-open system, and Closed system). By change in the
 190 combination of these factors, different degrees of the surface roughness could be effectively obtained
 191 as can be seen from Fig.6. Some phenomena caused by increase in the oxygen content of Si-Al-C-O
 192 fiber are shown as follows. As the oxygen content in the law fiber increases, the degradation reaction
 193 becomes faster. It easily leads to nearly stoichiometric composition of the degraded fiber. In this
 194 case, the partial pressure of CO gas on the surface of the fiber becomes higher compared with that of
 195 the other fiber with lower oxygen content. This leads to lower reaction rate at the surface of the fiber.
 196 Consequently, increase in the oxygen content of the raw Si-Al-C-O fiber led to decrease in the SiC
 197 crystalline size at the surface region. This means getting smooth surface. That is to say, the higher
 198 oxygen content of the raw Si-Al-C-O fiber and the closed system cause relatively higher CO content
 199 in the reactor during the degradation reaction, and then the consequently higher partial pressure of
 200 the formed CO gas at the surface region reduces the reaction rate to result in getting smooth surface.

201 Changes in the actual surface roughness of the obtained SiC-polycrystalline fibers, which were
 202 synthesized by heat-treatment at 1900°C in argon gas atmosphere using different raw fibers and
 203 different vessels, are shown in Fig.7.



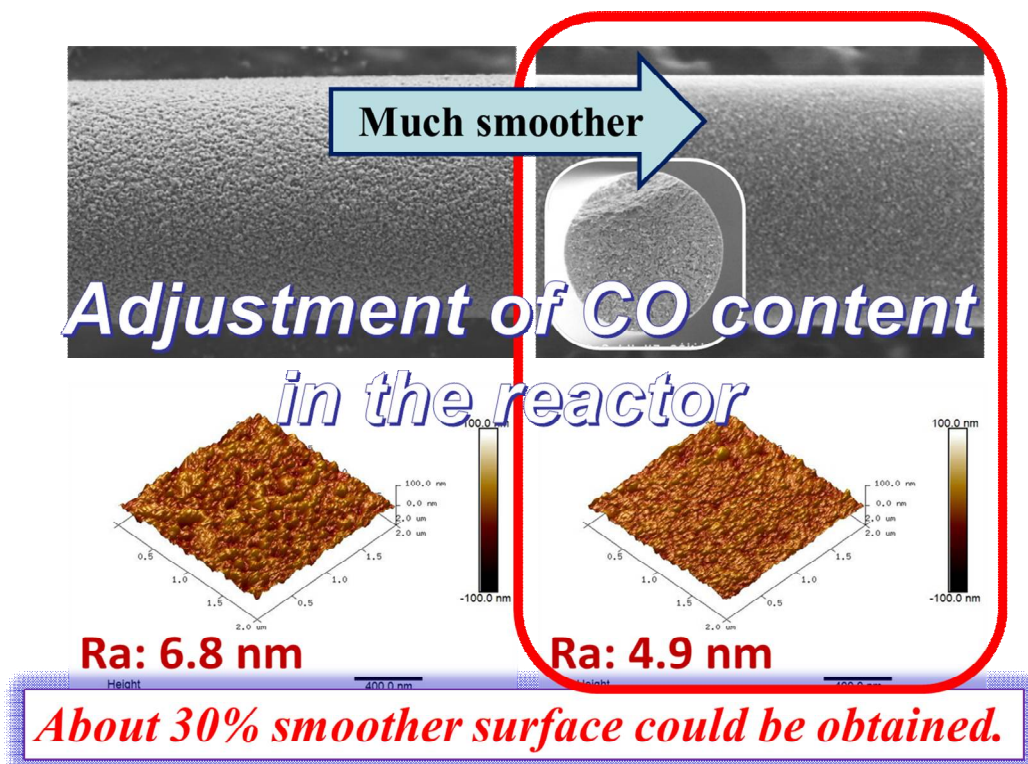
204

205 Fig.7 Change in the surface roughness of the SiC-polycrystalline fiber synthesized from
 206 different raw Si-Al-C-O fiber with different oxygen content at 1900°C in argon atmosphere. For
 207 obtaining A1, B1, C1, the raw fiber composed of $\text{Si}_{1.1}\text{Al}_{0.01}\text{C}_{1.5}\text{O}_{0.4}$ was used. For obtaining A2,
 208 C2 and for obtaining A3, B3, C3, the raw fibers composed of $\text{Si}_{1.1}\text{Al}_{0.01}\text{C}_{1.5}\text{O}_{0.45}$ and $\text{Si}_{1.1}\text{Al}_{0.01}\text{C}_{1.5}\text{O}_{0.5}$
 209 were used, respectively

210 As can be seen from this figure (Fig.7), the surface roughness could be controlled by changing
 211 both oxygen content of the raw Si-Al-C-O fiber and the reaction vessel. In this case, for obtaining A1,
 212 B1, C1 in Fig.7, the raw fiber composed of $\text{Si}_{1.1}\text{Al}_{0.01}\text{C}_{1.5}\text{O}_{0.4}$ was used for the synthesis. And, for
 213 obtaining A2, B2, C2 and for obtaining A3, B3, C3, the raw fibers composed of $\text{Si}_{1.1}\text{Al}_{0.01}\text{C}_{1.5}\text{O}_{0.45}$ and
 214 $\text{Si}_{1.1}\text{Al}_{0.01}\text{C}_{1.5}\text{O}_{0.5}$ were used, respectively. As can be seen from Fig.7, we could control the surface
 215 roughness from 67.99nm (maximum value) to 9.05nm (minimum value).

216 In this research, we used degradation process of the amorphous raw fiber (Si-Al-C-O fiber)
 217 accompanied by a release of CO gas and the subsequent sintering process, and also showed the
 218 controllable SiC crystalline size constructing the obtained SiC-polycrystalline fiber by changing the
 219 CO gas partial pressure in the reactor. In consequence, we could control the surface roughness of the
 220 SiC-polycrystalline fiber using CO gas released from the raw fiber. However, this means that an
 221 intentional change in CO gas partial pressure in the reaction vessel can lead to preferable crystalline
 222 structure.

223 **Fig.8** shows an improvement result regarding the surface roughness achieved by the
 224 adjustment of the CO gas partial pressure in the reactor during the degradation reaction. In this case,
 225 using Le Chatelier's principle, we accelerated the following reaction ($\text{SiO}_2+3\text{C}=\text{SiC}+2\text{CO}$) to
 226 consequently increase the CO gas partial pressure at the surface region of the fiber in the initial
 227 degradation process. Regarding this degradation condition, we reported the detailed content in the
 228 previous paper [6].

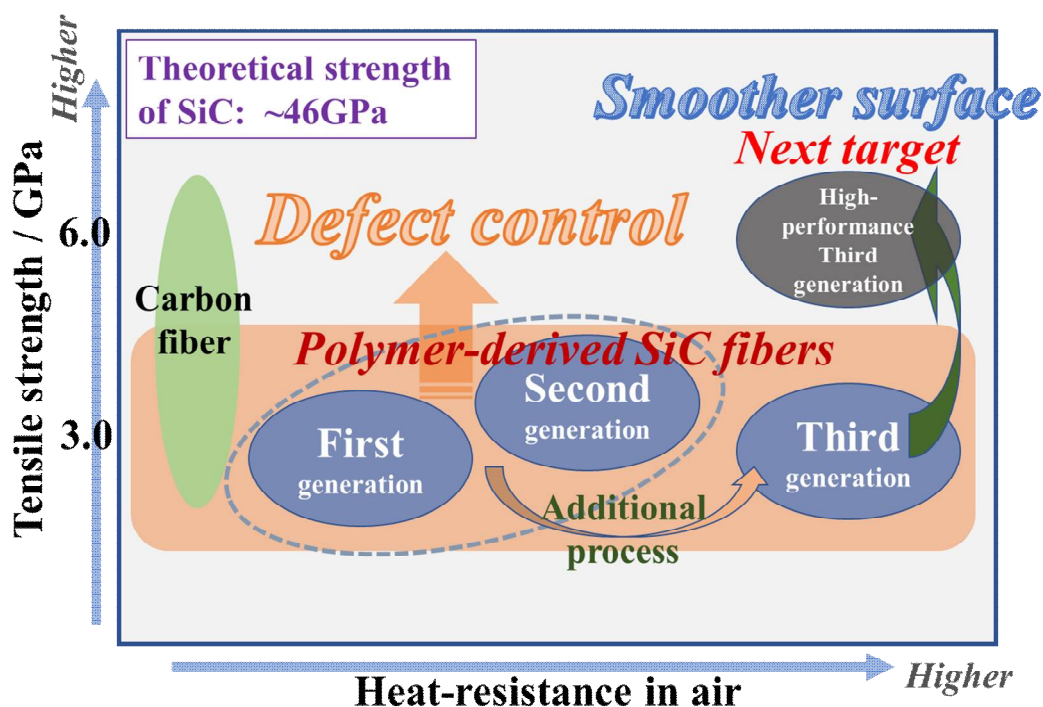


229

230 Fig.8 Improvement of the surface roughness by adjustment of CO content in the reactor

231 Finally, on the basis of our results, a perspective for developing the high-performance
 232 SiC-polycrystalline fiber is shown in **Fig.9**. Our target strength will be 6GPa, which is a similar
 233 strength to that of high-performance carbon fiber (T-800). To achieve the higher strength, the most
 234 important thing is to reduce the inside defects and surface roughness by controlling the partial
 235 pressure of CO gas in the reactor during the degradation reaction of the raw amorphous fiber.

236



237

238

Fig.9 Perspective for the high-performance SiC-polycrystalline fiber

239

4. Conclusions

240

241

242

243

244

245

246

247

248

249

250

251

252

253

Acknowledgments

254

255

This study was funded by a Grant from NEDO (New Energy and Industrial Technology Development Organization) via Ube Industries, Ltd. We gratefully acknowledge this financial support.

256

References

257

258

259

260

261

262

263

264

1. T.Ishikawa, Y.Kohtoku, K.Kumagawa, T.Yamamura, and T.Nagasawa, "High-strength alkali-resistant sintered SiC fibre stable to 2200°C", *Nature*, 391 (1998) 773-775.
2. M.Takeda, A.Urano, J.Sakamoto, and Y.Imai, "Microstructure and oxidative degradation behavior of silicon carbide fiber Hi-Nicalon type S", *Journal of Nuclear Materials*, 258-263 (1998) 1594-1599.
3. T.Ishikawa, "Advances in Inorganic Fibers", *Advanced Polymer Science* (Springer-Verlag Berlin Heidelberg) 178 (2005) 109-144.
4. J.J.Sha, T.Nozaawa, J.S.Park, Y.Katoh, and A.Kohyama, "Effect of heat treatment on the tensile strength and creep resistance of advanced SiC fibers", *Journal of Nuclear Materials*, 329-333 (2004) 592-596.

- 265 5. K.Itatani, K.Hattori, D.Harima, M.Aizawa, and I.Okada, "Mechanical and thermal properties of
266 silicon-carbide composites fabricated with short Tyranno Si-Zr-C-O fiber", *Journal of Materials Science*, 36
267 (2001) 3679-3686.
- 268 6. H.Oda and T.Ishikawa, "Microstructure and mechanical properties of SiC-polycrystalline fiber and new
269 defect-controlling process", *International Journal of Applied Ceramic Technology*, 14 (2017) 1031-1040.
- 270 7. T.Ishikawa and H.Oda, "Defect control of SiC polycrystalline fiber synthesized from
271 poly-aluminocarbosilane", *Journal of European Ceramic Society*, 35 (2016) 3657-3662.
- 272 8. T.Ishikawa and H.Oda, "Structural control aiming for high-performance SiC polycrystalline fiber",
273 *Journal of the Korean Ceramic Society*, 53(6) (2016) 615-621.
- 274 9. R.Usukawa, H.Oda, and T.Ishikawa, "Conversion process of amorphous Si-Al-C-O fiber into nearly
275 stoichiometric SiC polycrystalline fiber", *Journal of the Korean Ceramic Society*, 53(6) (2016) 610-614.
- 276 10. X.Zhao, R.M.Langford, I.P.Shapiro, and P.Xiao, "Onset plastic deformation and cracking behavior of
277 silicon carbide under contact load at room temperature", *Journal of the American Ceramic Society*, 94[10]
278 (2011) 3509-3514.
- 279 11. C.Sauder, A.Brussion, and J.Lamon, "Influence of interface characteristics on the mechanical properties of
280 Hi-Nicalon type-S or Tyranno-SA3 fiber-reinforced SiC/SiC minicomposites", *International Journal of*
281 *Applied Ceramic Technology*, 7(3) (2010) 291-303.
- 282